A SPATIO-SPECTRAL APPROACH FOR MOVEMENT DECODING FROM CORTICAL AND SUBCORTICAL RECORDINGS IN PATIENTS WITH PARKINSON'S DISEASE

Victoria Peterson*[1], Timon Merk[2], Alan Bush[1], Vadim Nikulin[3], Andrea A. Kühn[2], Wolf-Julian Neumann†[2] and Mark Richardson†[1]

[1]*Department of Neurosurgery, Massachusetts General Hospital, Harvard Medical School, Boston, United States.*

[2]*Movement Disorder and Neuromodulation Unit, Department of Neurology, Charité – Universitätsmedizin Berlin, Berlin, Germany.*

[3]*Department of Neurology, Max Planck Institute for Human Cognitive and Brain Sciences, Leipzig, Germany.*

Abstract: The application of machine learning to intracranial signal analysis has the potential to revolutionize deep brain stimulation (DBS) by personalizing therapy to dynamic brain states, specific to symptoms and behaviors. Machine learning methods can allow behavioral states to be decoded accurately from intracranial local field potentials to trigger an adaptive DBS (aDBS) system, closing the loop between patients' needs and stimulation patterns. Most decoding pipelines for aDBS are based on single channel frequency domain features, neglecting spatial information available in multichannel recordings. Such features are extracted either from DBS lead recordings in the subcortical target and/or from electrocorticography (ECoG). To optimize the simultaneous use of both types of signals, we developed a supervised online-compatible decoding pipeline based on multichannel and multiple recording site recordings. We applied this pipeline to data obtained from 11 patients with Parkinson's disease performing a hand movement task during DBS surgery targeting the subthalamic nucleus, in which in addition a research temporary ECoG electrode was placed. Spectral and spatial features were extracted using filter-bank analysis and spatial pattern decomposition. The learned spatio-spectral features were used to train a generalized linear model with sparse regularized regression. We found that movement decoding was successful using 100 ms time windows, epoch time that is well-suited for aDBS applications. In addition, when 9 out of 16 features were selected, decoding performance was improved up to 15% when the multiple recording site features were used as compared to the single recording site approach. The prediction value was inversely correlated with both the UPDRS score and the distance of the ECoG electrode position to the hand knob motor cortex. Further evaluation of the selected features revealed that ECoG signals contribute more to decoding performance than subthalamic signals. This novel application of spatial filters to decode movement from combined cortical and subcortical recordings is an important step toward the use of machine learning for the construction of intelligent aDBS systems.

Keywords: *adaptive Deep Brain Stimulation; Movement Decoding; Machine Learning; Invasive Neural Oscillation; Spatial Filters.*

*Corresponding author. vpeterson2@mgh.harvard.edu, Thier Building, 4th floor, Massachusetts General Hospital, 50 Blossom St., Boston, MA 02114.

†Equal contribution

1 Introduction

Deep brain stimulation (DBS) of the subthalamic nucleus (STN) or the globus pallidus internus (GPi) is an effective treatment for Parkinson's disease (PD) [1, 2]. Continuous high-frequency deep brain stimulation consistently improves the motor symptoms of PD patients [3]. Nonetheless, chronic stimulation of the brain has been shown to produce several side effects, such as dysarthria, dyskinesia and balance issues [4, 5]. In order to minimize the treatment side-effects, closed-loop or adaptive DBS (aDBS) guided by patient's electro-clinical state, has been proposed as a strategy to keep stimulation at a minimum [6]. The viability and success of these approaches strongly depends on the identification of reliable biomarkers reflecting patients' symptom severity and change with treatment, as well as on the computational strategies used for neural decoding.

For the development of aDBS, one promising strategy involves the detection of motor symptoms from intracranial electrodes implanted during DBS surgery. It has been shown that patient's behavioral neural biomarkers can be identified from local field potentials (LFPs) of the STN [7, 8]. Due to the functional coupling between subcortical and cortical structures [9, 10], the use of electrocorticography (ECoG) is being investigated for movement decoding [11, 12]. As an advantage, multichannel ECoG provides information of a broader area than STN recordings and are less affected by DBS-induced artifacts [13].

The most common approach for movement decoding from intracranial recordings is based on the extraction of band-power features at specific frequency ranges, such as in the beta ([13-30] Hz) and gamma ([30-100] Hz) bands, after band-pass filtering the signal. This strategy has been applied by several studies using either subcortical STN-LFPs [7, 8] or cortical ECoG signals [11, 14]. The combinational use of the LFP and ECoG signal has only recently been explored [15, 16]. Despite the type of signal used to perform decoding, the single band-power feature may limit the capability of the model to adapt to individual patient's needs.

The use of machine learning (ML) algorithms for brain decoding has largely been studied in the field of brain-computer interfaces (BCIs) [17]. The implementation of such methodologies within the field of aDBS may allow for the development of more sophisticated and subject-specific brain decoding algorithms [18]. Recent studies have shown how machine learning can be integrated in the context of aDBS [14, 19–21]. Interestingly, all these studies have based the decoding model in frequency-domain features extracted from a single frequency band. For boosting individual-performances, filter bank analysis can be performed [22, 23], and thus with a proper feature selection step, the most relevant frequency-band features can be identified. Additionally, most of the aforementioned approaches compute the frequency-domain features for each channel/sensor individually, neglecting the spatial information provided when working with multi-channels recordings.

Brain recordings are in most of the cases the consequence of electrical activity of neural populations sources firing in the proximity of the electrode. Unfortunately, due to the overlapping activity of multiple sources, such neural populations cannot be observed directly and must be inferred with uncertainty from their distorted recording representations [24]. Statistical generative models assume that brain signals arise from activity of uncorrelated sources, and that such sources appear geometrically distorted in the signal recording as a consequence of a linear mixing transformation, as illustrated in Figure 1.

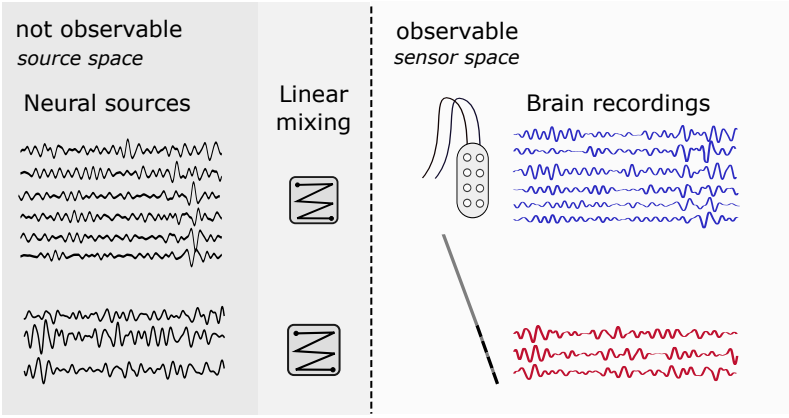

Figure 1: **Illustration of the generative statistical model in invasive neurophysiology.** The true neural sources are inferred by unobservable source space signals. These sources are mixed to constitute the sensor space signals (e.g. ECoG/STN-LFP). Spatial filters aim at estimating the sources by projecting the data in the sensor space to the source space

Spatial filtering methods aim to isolate the relevant spatial information embedded in multivariate (multichannel) signals. They directly work in the channel-time plane of the signal, capturing spatial relationships of the brain recordings. In the particular case of statistical spatial filters (Figure 1), the unobservable neural sources are estimated via decomposition of the multichannel brain recording, i.e., by demixing the observable brain signals.

The source power comodulation (SPoC) method [25] is a supervised spatial filter approach which allows to extract band-power related features correlated to a continuous output target signal. Therefore, SPoC is well suited to extract spatio-spectral features for identifying neural biomarkers related to movement, as recently showed in [26].

In this study, we constructed subject-specific ML-based invasive neurophysiology decoding models based on both the frequency and the spatial dimensions of the recorded brain activity, using a strategy that combines a filter-bank analysis with a spatial filtering approach. A multiple recording site (STN-LFP and ECoG) dataset from eleven (11) PD patients who performed a hand movement task during awake DBS implantation surgery was used. A generalized linear model (GLM) with Poisson regularized regression was implemented for predicting the movement. We evaluated regression performance of the model in two modalities: i) single recording site, in which either ECoG or STN LFP recordings were used as inputs to the decoding model and ii) multiple recording site, in which both ECoG and STN recordings were used together to learn the model. Since spatial filters were used, the neurophysiological interpretation of the solution was done, allowing a better understanding of how features and modalities contribute to movement decoding. We demonstrated that contralateral multiple recording site (ECoG + STN-LFP) recordings of 100 ms windows performs better than the single site approaches in predicting the force output, for both contralateral and ipsilateral movements. This study advances the use of ML methods with multivariate (multichannel) and multiple recording site recordings for the potential development of intelligent aDBS devices. The source code used throughout this work is available at GITHUB

2 Materials and methods

2.1 Data

The dataset used in this study (available upon request) corresponds to that from a previously published study [27] and is comprised of subthalamic LFP and subdural ECoG recordings simultaneously acquired from 11 PD patients (1 female, mean age $\pm$ SD = 60.1 $\pm$ 8.3 years, disease duration $\pm$ SD = 9.8 $\pm$ 4.0 years) undergoing DBS implantation surgery. All subjects were recommended for surgery by a multidisciplinary review board and provided written informed consent. The study was approved by the Institutional Review Board of the University of Pittsburgh (IRB Protocol #PRO13110420). UPDRS Part III scores for the off-medication conditions were collected in a time period of 1-3 months prior to surgery by movement disorder neurologists. Antiparkinsonian medications were held off for at least 12 hours prior to intraoperative testing.

Subjects were instructed to press a hand-grip force transducer with either their right or left hand after a visual cue appeared. A trial was considered successful if the subject was able to maintain for at least 100 ms with the indicated hand at least 10% of their maximum voluntary grip force. Each trial was followed by a variable inter-trial interval of 500–1000 ms. During the task, subjects were fully awake. No anesthetic agents were administered for at least 1 hour prior to the task procedure. No medication was given during the task.

ECoG recording were acquired using 6, 8, 28 or 32 contacts electrode strips (Ad-Tech, Medical Instrument Corporation), placed as close as possible to the hand knob area through the burr hole used for DBS lead implantation [28]. Ground and reference electrodes were placed in the shoulder and mastoid, respectively. LFPs from the STN were recorded using a clinical four contacts DBS lead (model 3389, Medtronic). Data was sampled at 1000 Hz and band-pass filtered (0.3–250 Hz), using a Grapevine neural interface processor (Ripple Inc.). STN-LFP data was re-referenced offline to a bipolar montage by referencing each contact to its immediate neighbor, thus three new bipolar channels were generated after this procedure.

All the analogical signals, corresponding to the grip-force output, were processed offline to remove baseline drift, by estimating the baseline using the optimization problem proposed in [29] and then subtracting it from the original output. After this procedure, the grip-force output was a continuous signal with zero (rest) or positive values (movement), where a value different from zero corresponds to the grip-force applied by the subject.

2.2 Spatio-spectral decomposition for movement decoding in PD patients

The proposed spatio-spectral pipeline for movement decoding in the context of invasive neuromodulation is depicted in Figure 2. The pipeline is designed to work in future real-time scenarios. Thus, simulated data packets (segments) of 100 ms were used to decode the incoming target sample. These recording segments, either from ECoG, STN-LFP or the combination of both, were decomposed into 8 well-defined frequency-bands, ranging from theta to gamma band. The SPoC method was then applied at each band, extracting only one spatio-spectral feature per frequency-band. Concatenated features were then used to feed a GLM to predict the target. In the following subsections details on the methods used to construct this framework are given.

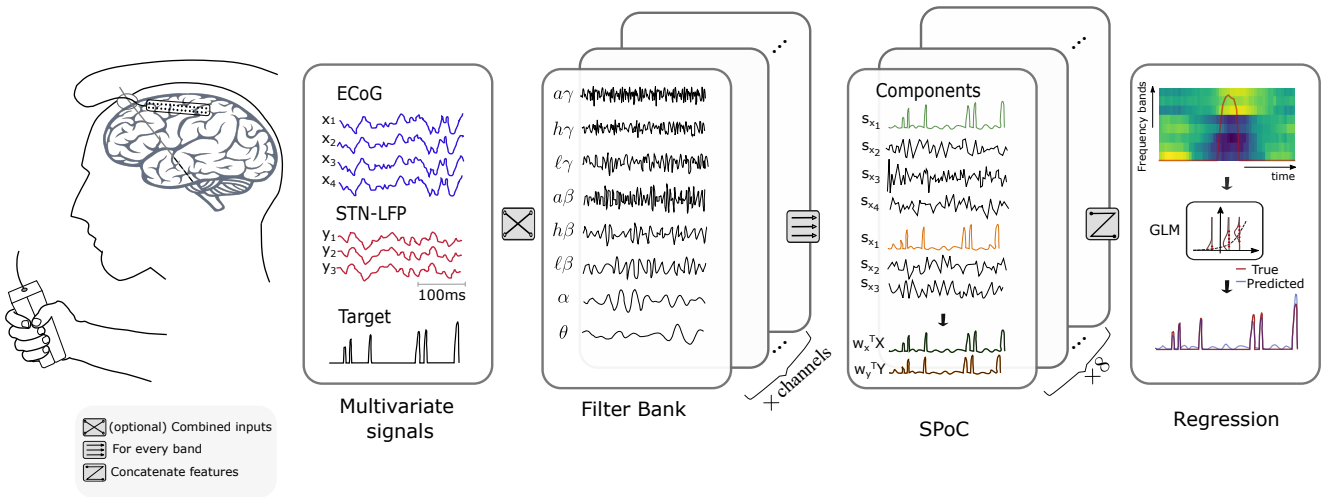

Figure 2: **Schematic representation of the proposed decoding pipeline.** Segments of 100 ms from the invasive multi-channel recording were decomposed in eight frequency bands. The supervised spatial filtering SPoC method was applied at each frequency band, extracting the source more correlated to the target variable. One spatio-spectral feature was extracted from each frequency band. Movement decoding was based on a GML regression model, in which a Poisson sparse penalized regularization was implemented.

2.2.1 Online-compatible data pre-processing

Considering real-world applications, pre-processing steps should account for online real-time decoding challenges, that is, data is only available in packets, and future packets from the time point of decoding are not available to the decoder or processing pipeline. Thus, in this work, consecutive epochs of 100 ms were extracted from the brain recording in order to continuously decode the grip-force target. Common average reference was applied to the extracted ECoG segments. All epochs were notch (60/120/180 Hz) and band-pass filtered in eight frequency bands of interest θ : [4-8] Hz, α: [8-12] Hz, lowβ: [13-20] Hz, highβ: [20-35] Hz, allβ [13-35] Hz, lowγ: [60-80] Hz, highγ: [90-200] Hz, and allγ: [60-200] Hz). The pre-processed brain recordings were arranged in a four-dimensional array accounting for the number of extracted epochs N_t, the number of channels N_c, the numbers of sample point per epoch N_s and the number of filter-bands N_f. In the case of the target variable, in accordance with the 100 ms time window length, we downsampled each by 100 samples.

2.2.2 Feature extraction via source power comodulation

Electrophysiological recordings can be modeled as a linear and instantaneous superposition of neural sources [30, 31]. Let $\mathbf{x}(t) \in \mathbb{R}^{N_c}$ be the brain recordings in the sensor space (raw data) at time t, where N_c denotes for the number of channels. Let $\mathbf{s}(t) \in \mathbb{R}^{N_c}$ be the sources (or components) and let $\mathbf{A} \in \mathbb{R}^{N_c \times N_c}$ be the mixing matrix, whose i^{th} column vector $\mathbf{a}_i$ is what is known as *spatial pattern*. Considering additive noise, the following definition holds to represent the generative model:

$$\mathbf{x}(t) = \mathbf{A}\mathbf{s}(t). \tag{1}$$

In the context of spatial filtering, the objective is to estimate $\mathbf{s}(t)$ and thus, transform the signal from the *sensor* to the *source* space. This sensor-to-source transformation can be obtained by means of the so-called blind source separation methods, as follows:

$$\hat{\mathbf{s}}(t) = \mathbf{W}^T \mathbf{x}(t), \tag{2}$$

where $\mathbf{W} = [\mathbf{w}_1, \ldots, \mathbf{w}_i, \ldots, \mathbf{w}_{N_c}]$ is a $N_c \times N_c$ demixing matrix whose i^{th} column vector corresponds to what is known in the literature as *spatial filter*. Each of the spatial filter is meant to extract the signal from one source while suppressing the activity of the others, such that the resulting projected signal is a close approximation of the original source signal [25]. In the particular case of the SPoC algorithm, method simultaneously discovered by [25, 32], the information contained in the outcome variable is used to guide the decomposition. Denoting $\mathbf{z}(t)$ to the target variable (grip-force movement), the first SPoC filter is found by:

$$\mathbf{w}_{spoc} = \underset{\mathbf{w} \in \mathbb{R}^{N_c}}{\arg\max} \frac{\mathbf{w}^T \mathbf{C}_z \mathbf{w}}{\mathbf{w}^T \bar{\mathbf{C}} \mathbf{w}}, \tag{3}$$

where $\bar{\mathbf{C}} = \frac{1}{N_t} \sum_i^{N_t} \mathbf{C}_i$ is the Euclidean average covariance matrix across the N_t data segments and $\bar{\mathbf{C}}_z = \frac{1}{N_t} \sum_i^{N_t} z_i \mathbf{C}_i$ is the weighted average covariance matrix. The rest of the filters are obtained by solving a generalized eigenvalue decomposition problem [25]. As shown in [24], the matrix $\mathbf{W}_{spoc}$ recovers the inverse of mixing matrix $\mathbf{A}$ defined in (1).

When data has been band-pass filtered, the power of the projected signal $\mathbf{w}^T \mathbf{x}(t)$ approximates the target function $\mathbf{z}$. Thus, after applying SPoC spatio-spectral features can be extracted by $var\left[\mathbf{w}^T \mathbf{x}(t)\right]$. If the subsequent decoding model assumes linear relationships between the input and the output, the logarithm of the extracted features are then taken. In this work, the SPoC method was applied at each frequency band considered, leading to eight (8) spatio-spectral features. It is timely to mention here that while offline learning of the spatial filters $\mathbf{W}_{spoc}$ is needed, once such a matrix is learned, the spatio-spectral features can be extracted in real-time by the proper signal projection.

2.2.3 Generalized regularized linear models

Let $\mathbf{H} \in \mathbb{R}^{N_p \times N_t}$ be the matrix of N_p predictors (features), where N_t is the number of extracted epochs. Let $\mathbf{z} \in \mathbb{R}^{N_s}$ be as before, the target variable. Traditional linear model assumes that the distribution of the output is normal ($\mathbf{z} \sim \mathcal{N}$) and thus, it can be modeled as a linear combination of the predictors and suitable weights, that is:

$$\mathbf{z} = \beta_0 + \boldsymbol{\beta}\mathbf{H} + \boldsymbol{\epsilon},$$

where the model parameters β_0, $\boldsymbol{\beta} \in \mathbb{R}^{N_p}$ can be estimated using ordinary least squares or its regularized versions. In the particular case of the elastic-net penalty (enet), a compromise between the ℓ_1 and ℓ_2 norm of the solution is imposed, and thus the solution vector and intercept can be found by solving the following unconstrained

regularized problem:

$$\min_{\beta_0,\boldsymbol{\beta}} \frac{1}{N}\sum_{i=1}^{N} \mathcal{L}(z_i, \beta_0 + \boldsymbol{\beta}^T h_i) + \lambda[\frac{1}{2}(1-\alpha)\|\boldsymbol{\beta}\|_2^2 + \alpha\|\boldsymbol{\beta}\|_1], \tag{4}$$

where $\mathcal{L}(\cdot)$ is the loss function aimed to be minimized and λ and α are positive constants called regularization parameters. In particular, $\alpha \in [0,1]$ and thus it balances between the Ridge regression ($\alpha = 0$) and LASSO regression ($\alpha = 1$).

When working with non-normally distributed outputs, we can extend this approach by means of generalized linear models (GLMs). The Poisson distribution is a discrete probability distribution that expresses the probability of a given number of events occurring in a fixed interval of time. Since the grip-force target is a non-negative output which accounts for rest and movement events, we assume here, from practical reasons, that $\mathbf{z}$ can be modeled as coming from a Poisson distribution. Under this assumption, a $\log$ - $\exp$ relationship between the predictors and the output exits, and the loss function $\mathcal{L}(\cdot)$ in (4) is given by:

$$\mathcal{L}(\beta_0, \boldsymbol{\beta}) = \sum_i \left\{ z_i \log(\kappa_i) - \kappa_i \right\}, \qquad \text{with} \quad \kappa_i = \log(1 + \exp(\beta_0 + \boldsymbol{\beta}^T h_i)). \tag{5}$$

3 Results

In order to investigate the practical use of the spatial filters for the development of aDBS, different analytical experiments were conducted. Since the dataset comprises bilateral movements (contra- and ipsilateral to the electrodes' position on the respective hemisphere), one decoding model was built for each subject at each movement laterality. A 5-fold non-shuffled cross-validation procedure was performed, where the coefficient of determination R^2 was used for measuring the performance of the predicted grip-force when compared to the true grip-force output. The SPoC algorithm was applied as a feature extraction method at each frequency band considered. The demixing matrix W_{spoc} was learned using the training set in each cross-validation fold, and features from the unseen testing set were extracted using these estimated filters. One spatial filter was used to compute the feature at each frequency band, leading to eight spatio-spectral features at the end of the filter-bank analysis. Features were concatenated and z-score scaled. In order to avoid any circularity, the statistics (mean and standard deviation) were estimated in the training set and then applied to scale the unseen testing test. These features corresponded to the inputs to the Poisson-GLM with enet penalty regression model. In order to equally balance the Ridge and Lasso penalty, we set the α parameter of (4) equal to 0.5. The regularization parameter λ was searched via Bayesian Optimization [33] over a 3-fold cross-validation on training data. Statistical analyses were performed via the non-parametric Friedman test and the post-hoc Nemenyi test at level of significance 0.05.

The simulations as well as the corresponding Python source codes developed for this work are publicly available at GITHUB. We used the MNE library [34] for implementing SPoC, the pyglmnet package for running the GLM [35], a modified version of the FilterBank function of the MOABB library [36] for extracting the spatio-spectral features within a scikit-learn pipeline [37], and the Bayesian Optimization package [38] for finding the optimal regularization parameter.

3.1 ACCURATE MOVEMENT DECODING IS ACHIEVED WITH 100MS TIME WINDOWS SEGMENTS

Contra- and ipsilateral hand movement was decoded from ECoG and STN-LFP signals combining a filter-bank spectro-spatial feature extraction method with a generalized linear model (see Section 2.2). While 100 ms was the window length adopted to extract the spatio-spectral features, by means of a Wiener filter [39] approach, the contribution of different features concatenated over time can be investigated, as shown in [21, 40]. In this sense, we investigated the impact in decoding performance when adding features from previous time segments, ranging from 100 to 1000 ms in steps of 100 ms. The decoding model was evaluated at each time concatenation considered. The feature vector, input to the GLM model, was the result of stacking the 8 spatio-spectral features coming from each time window. Thus, while for the 100 ms time window, only 8 features were used as inputs to the regression model, in the 1000 ms time window the dimension of the feature vector was 80 (8 spatio-spectral features $\times$ 10 time-windows). This analysis was made on both the ECoG and the STN-LFP recordings. The overall results are shown in Figure 3.

Several findings were noted. First, decoding based on ECoG recording was consistently better than that based on STN-LFP signals. Second, a decoding model based on contralateral movements performed better than its ipsilateral counterpart. Third, for this spatio-spectral GLM-Poisson decoding model, adding features from previous time windows did not further improve performance (p-value ≥ 0.4). In fact, although for both brain recordings and movement lateralities the maximum R^2 value was found around 300 ms (mean R^2 ECoG contralateral: 0.18, mean R^2 STN-LFP contralateral: 0.12, mean R^2 ECoG ipsilateral: 0.11, mean R^2 STN-LFP ipsilateral: 0.08), the statistical analysis against those values in the 100 ms time window (mean R^2 ECoG contralateral: 0.16, mean R^2 STN-LFP contralateral: 0.11, mean R^2 ECoG ipsilateral: 0.10, mean R^2 STN-LFP contralateral: 0.07) indicated that this gain was not significant (p-value ≥ 0.4).

In order to further characterize the impact in decoding performance when working with spatio-spectral features extracted from a specific time window, the coefficient values of the regularized solution vector, output of the GLM model, were analyzed. Since sparsity was imposed in the solution via LASSO regularization (see Eq. (4))), a coefficient value equal to zero in the GLM model indicates that the associated feature was not relevant for the decoding viewpoint. The average coefficient value across subjects for each signal recording and laterality is shown in Figure 4. As can be observed, coefficients beyond the 100 ms time window are close or equal to zero. In addition, ECoG associated coefficient values are higher than those from the STN.

Given the lack of significant effects found across time concatenated windows and the solution coefficient values observed, for the following experiments our decoding model was based on segments of the first 100 ms.

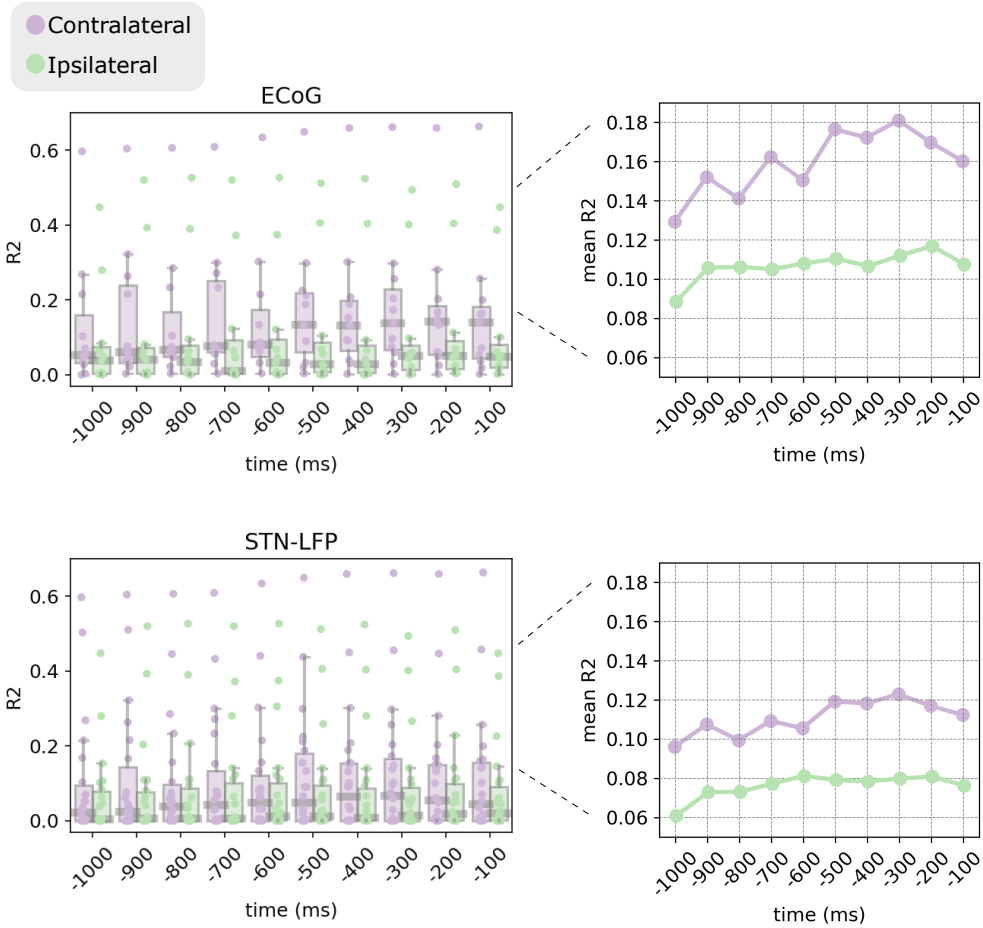

Figure 3: **No significant improvement of movement decoding with increased number of 100ms time windows.** Ranging from 1000 ms to 100 ms, the decoding model was trained using the concatenated spatio-spectral features up to the indicated time window. Decoding performance yielded by ECoG (top) and STN-LFP (bottom) recordings are presented separately. For each type of recording site, contralateral and ipsilateral movements decoding are shown in violet and green color, respectively. The figures on the left aggregates the mean R^2 across subjects at each time concatenation considered.

3.1.1 Combining cortical and subcortical data

ECoG and STN-LFP signals were recorded simultaneously in these subjects. Since cortical activity is synchronized with the subthalamic oscillations, a multiple recording site decoding model can be built by combining these two brain recordings modalities. In order to investigate if such multiple recording site approach can gain performance compared to the single site models, the spatio-spectral features vector of ECoG and STN-LFP were combined. Since the spatio-spectral features were extracted from the 8 frequency bands, the dimension of the resulting multiple recording site vector is 16 (8 features per modality). Figure 5a shows the performance of the decoding model using ECoG + STN-LFP recordings against decoding models that only use either ECoG or STN data. The statistical analysis indicated that there are no significant differences between the multiple recording site ECoG + STN-LFP decoding model and the ECoG decoding model (p-value=0.9).

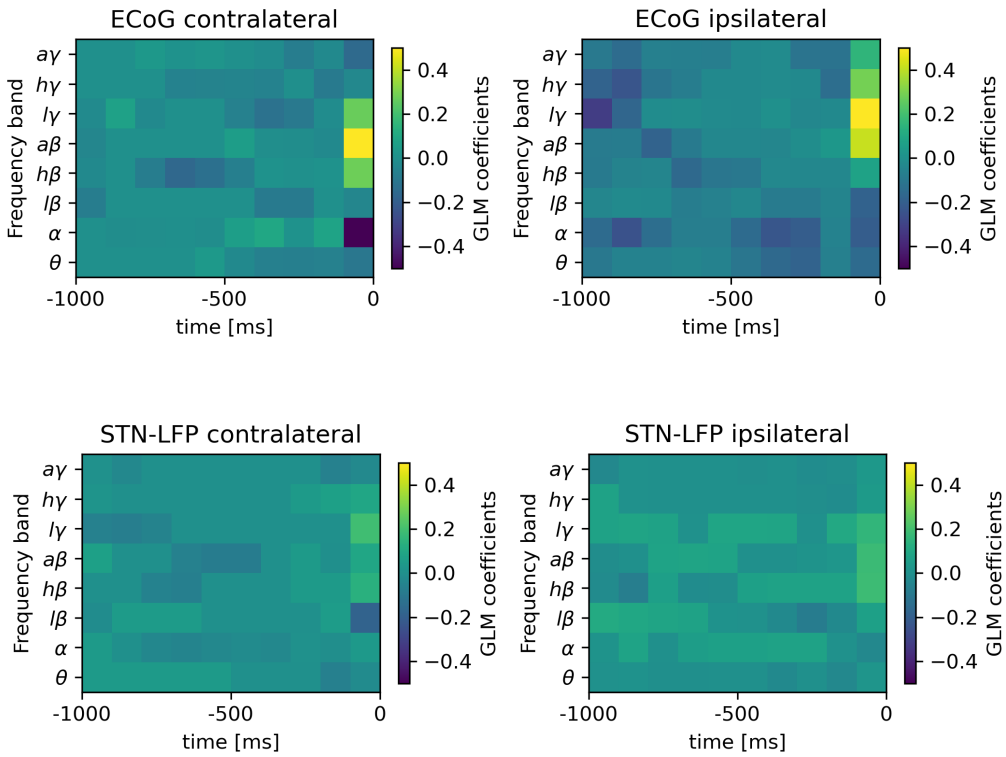

Figure 4: **Features used for movement prediction are dominated by features calculated in the last 100ms time window.** For each brain recording and movement laterality we explored the coefficient value of the GML solution vector over the 5-folds. Due to the nature of the Poisson distribution, for better interpretation of the output, the coefficient values were transformed by taking the exponential and then changing their sign. For the sake of comparison across different subjects and cross-validation outputs, a normalization step (between -1 and 1, avoiding zero entries) was applied to each coefficient matrix in the frequency-time plane. Plots show the grand-average coefficient values across subjects.

Figure 5b and 5c show how the performance of the multiple recording site approach correlates with the total UPDRS III score and the mean distance between the electrode location and the target area. Subjects from which the multiple recording site approach resulted in worse, equal or better than the single site ECoG approach are depicted by different colors and dots sizes. The Pearson correlation coefficient, shown in the top right side of each subplot, indicates that negative correlation exists between the yielded performance and the UPDRS score and electrode grid distance to the hand knob area.

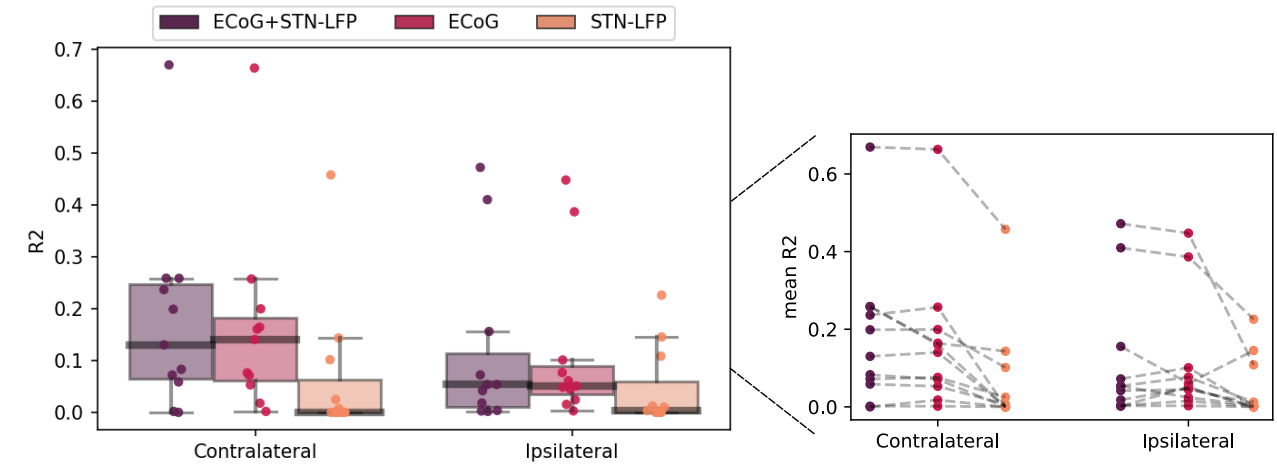

(a)

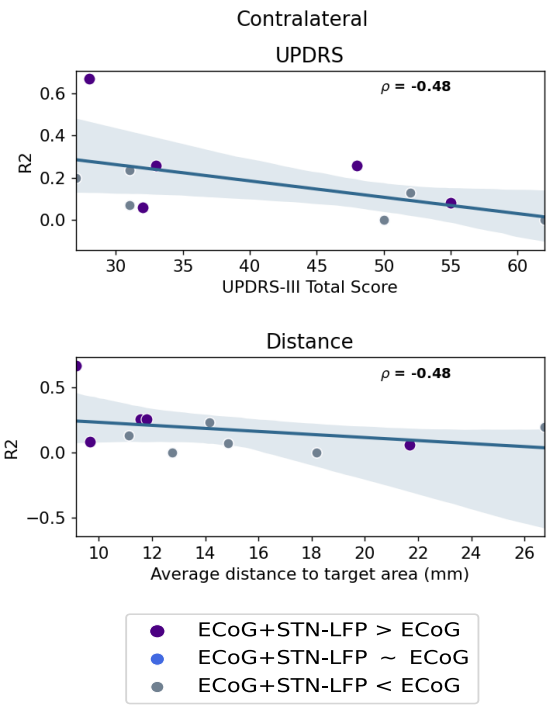

(b)

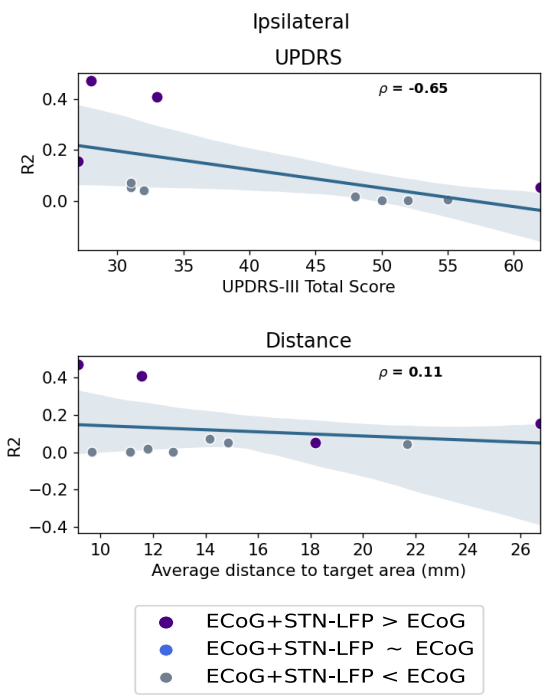

(c)

Figure 5: **Adding STN-LFPs features does not significantly improve ECoG-based decoding.** a) Performance comparison between multiple recording site and single recording site approaches. The performance in decoding contralateral and ipsilateral decoding is shown separately. The plot on the right links decoding performance across the same subject (dot) when using STN, ECoG and ECoG + STN-LFP data. b) Correlation between the multiple recording site performance and i) the UPDRS score ii) the distance to the target area, for the contralateral movements. c) Correlation between the multiple recording site performance and i) the UPDRS score ii) the distance to the target area, for the ipsilateral movements Subjects are colored according to the multiple recording site performance gain with respect to the ECoG approach.

3.1.2 Neurophysiological interpretation of the solution

The use of spatial filtering methods to decompose the brain signal allows for a neurophysiological interpretation of the solution [41]. The topographic plot of the spatial patterns, i.e. the column vector of the matrix **A** introduced in Section 2.2.2, may illustrate how the brain activity is expressed in the measured channels. The proposed spatio-spectral decoding method based on a sparse GLM yields solution vectors with a small number of non-zero entries. As indicated before, these non-zero coefficients represent the selected features for building the decoding model. When working with multisite data, it is interesting to see which spatio-spectral features were selected from each brain recording modality. This is shown in Figure 6a for the subject achieving the highest contralateral decoding performance. Interestingly, for this particular subject, the decoding model depends on spatio-spectral features coming from both cortical and subcortical electrodes. The spatial pattern associated to each frequency band feature is shown in Figure 6b.

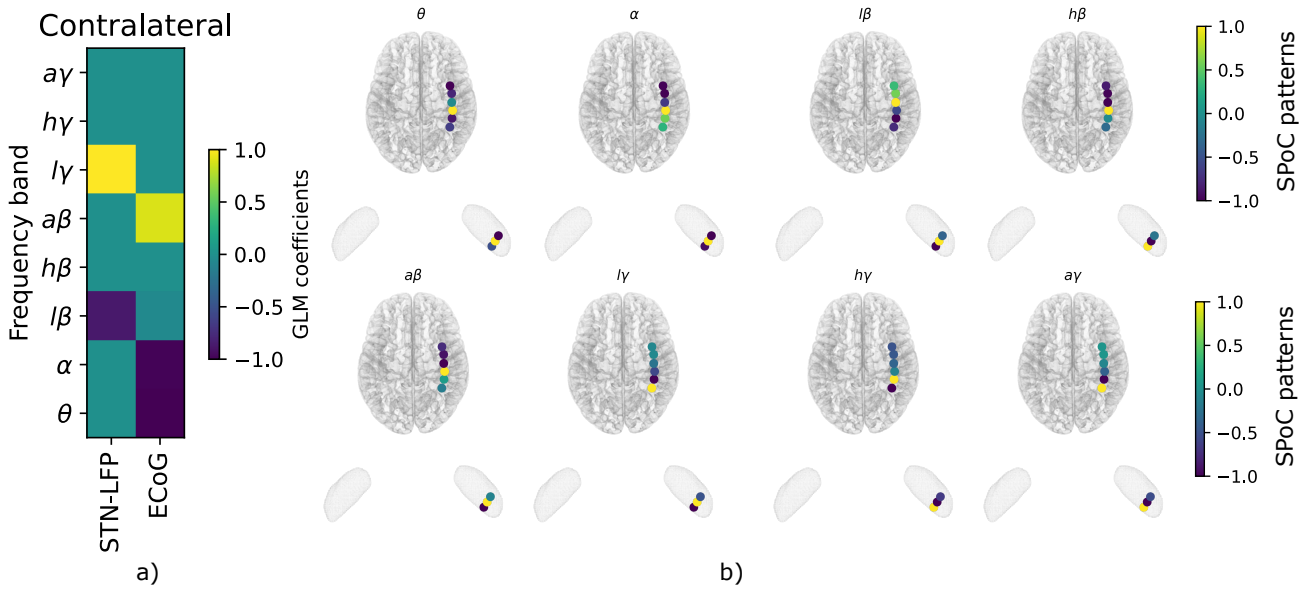

Figure 6: **Spatio-spectral information.** For a given subject (S01), the mean coefficient values across folds is shown as well as the associated spatial patterns at each frequency band considered. As before, coefficients were appropriately transformed and normalized before taking the average across cross-validation folds. For illustration purposes, the spatial patterns are normalized between -1 and 1.

3.2 More restrictive feature selection renders multiple recording site decoding better than single recording site

The combination of the spatio-spectral features of the two brain recording modalities comes along to the cost of working on a higher dimensional space as compared to the single recording site approaches. Thus, to understand the impact of sparsity to the solution vector in decoding performance, an imposed dimensionality reduction experiment was conducted.

When working with sparse regularized models, the degree of freedom of the solution, i.e., the number of non-

zero coefficients in the solution vector, is highly correlated with the value of the regularization parameter λ. It is well known that for a given value of λ, called λ_{max} all coefficient values are equal to zero. In the extreme scenario, all coefficients will be non-zero when $\lambda \rightarrow \lambda_{\text{min}}$, i.e. the value of λ at which the sparsity constrain is neglectable. Thus, in order to impose different degrees of freedom in the solution, the regularization parameter was set at different values between λ_{max} and λ_{min}. As before, the balancing parameter α in the elastic net formulation presented in (4) was set equal to 0.5. Figure 7a shows the mean R^2 value across subjects at different degrees of freedom values in the solution.

In order to analyze which features were most commonly selected at the point of maximum mean R^2 value, the overall coefficient values across subjects are shown in Figure 7b. Note that while for contralateral movement there is a tendency of keeping only ECoG features in the model, in the ipsilateral case both STN and cortical signals are retained for the decoding.

Figure 7c shows the comparison between the single recording site approaches and the multiple recording site approach at the point of maximum mean R^2 depicted in Figure 7a. In this scenario, the mean contralateral decoding performance gain of the multiple recording site approach with respect to the ECoG and the STN-LFP is about 5.2% and 14.9%, respectively, achieving up to 0.7 of R^2 for the best subject. The statistical test indicated that such improvements are significant for the STN-LFP (p-value = 0.001).

4 Discussion

In this work we developed a spatio-spectral approach to decode movement using invasive brain recordings in patients with Parkinson's disease. The supervised spatial filter SPoC method was used to extract features at eight pre-defined frequency bands. The predictive model was built via GLM with regularized Poisson sparse regression. Several analyses were conducted, taking into consideration compatibility with future online restrictions.

The analysis of features coming from different 100 ms time-windows, revealed that adding features accounting for brain activity prior to the 100 ms time-window did not significantly contribute to the decoding performance. Although other studies have shown that adding features form previous time-segments could improve decoding [21, 40], those studies based their analyses on regression models assuming a Gaussian distribution. Our use of a non-negative distribution could explain why we did not observe any improvement with adding more features to the model. The resting period was thought to be characterized best by a non-negative distribution, given that it was the most frequent state in the target variable, whose values were represented as zero-grip force. Along these lines, when analyzing the coefficient values of the GLM across the different time-points and subjects, the coefficient values plots revealed that features coming from time-windows prior to 300 ms tended to not be selected by the model. Thus, no linear combination between the features could be found to explain the target output. This phenomena is also easy to observe in Figure 4, where the grand-average of the coefficient values across subjects show that the most relevant features are generally selected from the 100 ms time segment. Interestingly, the associated coefficient value for the STN-LFP signal is always lower compared to the ECoG signal. This is in line with the difference in performances reached by each signal modality, as depicted in Figure 3.

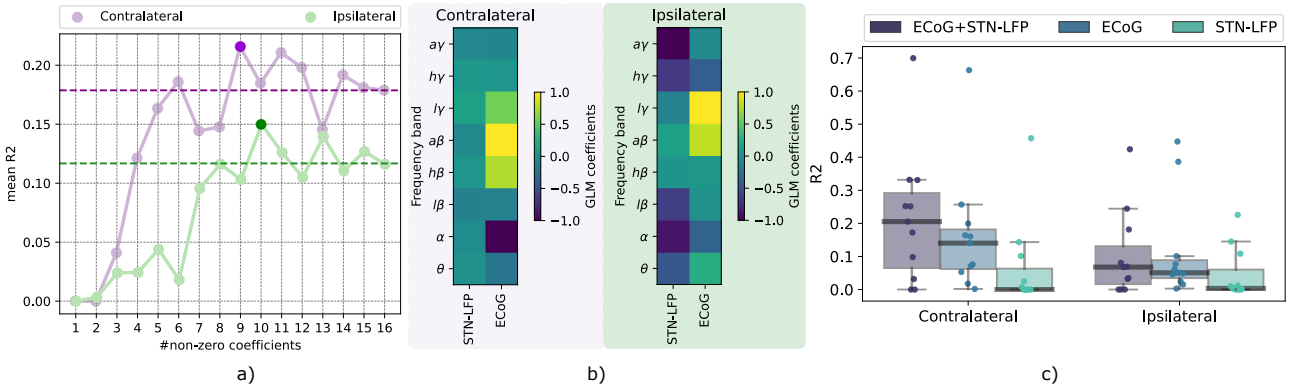

Figure 7: **Imposed feature dimension improves movement decoding for the multiple recording site approach.** To evaluate which features seem to be more representative when ECoG and STN-LFP data is jointly being used, we imposed different degree of sparsity in the solution. a) Impact on performance as the sparsity in the solution decreases. Results are desegregated between contralateral and ipsilateral movements. Dashes lines show the mean R^2 value achieved in the previous experiment with the multiple recording site approach at each movement laterality. The value at which the performance reached its maximum is highlighted with the colored dots. b) Grand-average across-subjects of the coefficient values for the best contralateral (#non-zero coefficients equal to 9), and ipsilateral model (#non- zero coefficients equal to 10). As before, normalization was applied before taking the mean across cross-validation folds and subjects. c) Decoding performance of the combined ECoG + STN-LFP approach at the optimal number of features as compared to the single recording site approaches. The overall mean gain of the multiple recording site approach is 5.2% and 14.9% with respect to single ECoG and STN-LFP models, respectively.

The superiority of ECoG over STN-LFP for movement decoding can also be observed in Figure 5a. These findings are in line to what was found in [21], and could be explained by the fact that ECoG recordings have a better spatial resolution (more electrode contacts), provides a much stronger signal and allow the measurements of high amplitude oscillations than depth recordings [42]. The combination of ECoG and STN recordings for building the decoding model resulted in similar performance to when only ECoG signals were used (Figure 5). Upon detailed inspection of these results, it can be observed that performance was often reduced when using ECoG + STN-LFP as compared to only using ECoG. To better understand this result, ECoG + STN-LFP performance was correlated with the UPDRS score and the distance of the electrodes to the target area (see figures 5b and 5c). We found that better accuracy was obtained using data from subjects with less severe disease (lower the UPDRS score), and from electrode locations closest to the presumed center of the motor territory of each target.

One of the main advantages of using blind-source separation methods for finding the neural sources is that the solution is neurophysiologicaly interpretable. Since a linear model was used to learn the mapping between the features and the movement target output, the coefficient values of the solution can be correlated to feature importance. Figure 6a shows the coefficient values associated to each spatio-spectral feature across the different brain modalities and frequency bands, for the subject with the highest accurate prediction. For this subject, only

6 out of 16 features were relevant for building the decoding model. Since spatial filters were used to extract those features, we could investigate the neural activity at each electrode location in each frequency band, by plotting the corresponding spatial pattern (Figure 6b). If we analyze those patterns corresponding to the selected features by the model, we can see that the most relevant ECoG features correspond to those patterns exhibiting stronger low frequency desynchronization (see spatial patters for $\theta, \alpha, a\beta$). A similar analysis can be made in the case of STN, in which, the chosen features show a similar activation pattern map (see spatial patters for $l\beta$ and $l\gamma$).

The automatically selection of regularization parameters is still an open issue in the community. Different strategies exit to alleviate the process of finding the optimal hyperpatemeter of a model. Here, the Bayesian optimization was used to automatically select the λ regularization parameter in the enet GLM. A further analysis of the impact in performance of the number of non-zero coefficients in the solution was performed. For doing so, a range of pre-defined λ values was set so as to get solutions with desired degrees of freedom. The results, presented in Figure 7a, show that overall performance of the multiple recording site approach can be improved when the number of non-zero coefficients is chosen to be around 9 and 10 (previous decoding performance shown in horizontal lines). This approach also revealed a gain compared to the single recording site approaches (see Figure 7c), in line with promising results recently reported using combinations of ECoG and LFP for parkinsonsian motor symptom characterization in adaptive DBS [16]. Our results suggest that the combinational use of ECoG and STN-LFP can improve decoding performance and could lead to a more robust model of changes in such recordings. In this sense, the ECoG + STN-LFP approach would be expected to better account for data variability, selecting the best-performing ECoG or/and STN-LFP features at a given time.

By analyzing the plots of the selected features at optimal performance (Figure 7b), we can see that while for the contralateral case, the chosen features are generally being selected from the ECoG modality, for the ipsilateral case, this tendency is not observed. This can be explained by the fact that movement-related neural activity is not localized in the ipsilateral side as compare with the contralateral one: whereas in the contralateral side gamma band activity increases while beta band activity decreases in specific region of the motor area during movement, in the ipsilateral side spatially broad beta activation is observed.

The first uses of ML methods to build BCI models in the context of aDBS have recently emerged. Most of those studies based their analyses in single electrode approaches [19, 21]. In addition, extracted features are primarily spectral features, which then are used to feed a linear model. In this work we have constructed a decoding model based on both the spectral and the spatial information of the recording channels, gathering all the information collected throughout the several contacts at once. This represents a conceptual advantage over single-electrode approaches, since less processing time is needed (no need to process all channels and afterwards select the best one) and more robustness is gained diminishing channel decoding bias. In the context of adaptive DBS, different daily-life activities, such as speech and walking, should simultaneously be decoded. Considering such scenario, this type of spatial analysis could allow better discrimination between different behavioral states. Indeed, Jiang et al. [43] have shown that different spatial patterns could be observed for four types of movement tasks, and thus spatial filters could be used to differentiate between them. In addition, spatial filter methods also have been used

in the context of DBS with concurrent scalp electroencephalography, for both identifying neural markers related to movement and for detecting whether DBS stimulation was on or off [44].

In consideration of future real-time applications in the context of adaptive DBS, a 100 ms window was used to learn the model, achieving an overall decoding capacity of 0.22 R^2. This is extremely important when considering the need to decrease the buffer time needed to record the portion of data required within the decoding pipeline as much as possible.

Several limitations of this study are worth noting. First, we based our analyses on data obtained with a grip-force task, which describes just one type of motor behavior. Second, the data was recorded during the DBS implantation surgery, when participants were without medication, an otherwise unnatural state relative to typical condition. In addition, the DBS device was OFF. Given that such conditions change the state of recorded brain activity, further research is needed to account for such sources of variability. Lastly, our analytic experiments were based on a single session per patient. Considering the lack of stationarity in the electrophysiological brain data, future models ideally should be tested in several recording sessions, acquired at different days.

The proposed decoding pipeline can also be extended to use for real-time detecting other human behavior tasks, such as speech. The decoding capacity in this context as well as in online settings are part of future research plans.

5 Conclusions

We implemented a ML-based decoding pipeline for movement decoding in patients with Parkinson's disease, using simultaneously recorded cortical and subcortical LFPs as inputs. Using spatial filters for the first time to decode movement from intracranial data collected during DBS surgery, we extracted spatio-spectral features coming from eight frequency bands. We found that via the Poisson GLM there is no need to add features extracted from time segments prior to 100 ms, which has significant implications of the feasibility of online decoding. We showed that the combination of ECoG and STN recordings could improve the decoding in 5.2% as compared to when only ECoG was being used. The analysis of the model's coefficients indicated that while contralateral movements are generally well characterized with a few features, decoding ipsilateral movement will require more features originating from multiple locations and frequency bands. This work advances machine learning approaches for developing intelligent adaptive DBS therapy. Future studies will include the analysis of cross-subjects decoding via common spatial distribution functions, the decoding of other physiological and pathological states as well as online applications of the pipeline.

Author contribution

Victoria Peterson: Conceptualization, Methodology, Software, Validation, Formal analysis, Writing - Original Draft, Visualization. **Timon Merk**: Software, Data Curation, Writing - Review & Editing. **Alan Bush:** Conceptualization, Investigation, Data Curation, Writing - Review & Editing. **Andrea A. Kühn:** Conceptualization, Writing - Review & Editing, Project administration, Funding acquisition. **Vadim Nikulin:** Conceptualization,

Methodology, Writing - Review & Editing. **Wolf-Julian Neumann:** Conceptualization, Writing - Review & Editing, Supervision, Project administration, Funding acquisition. **Mark Richardson:** Conceptualization, Investigation, Writing - Review & Editing, Supervision, Project administration, Funding acquisition.

DECLARATION OF INTEREST

The authors declare no conflict of interest. The funders had no role in the design of the study; in the collection, analyses, or interpretation of data; in the writing of the manuscript, or in the decision to publish the results.

ACKNOWLEDGMENTS

We would like to thank the subjects for their generous gift of time in the operating room and additional experimenters who acquired and organized the data. In addition, we would like to thank Denis A. Engemann for suggesting the use of a generalized linear model with non-negative distributions. The present manuscript was supported through a US-German Collaborative Research in Computational Neuroscience (CRCNS) grant, funded by the Federal Ministry for Research and Education (Germany) and the National Institutes of Health (United States, R01NS110424). In addition this manuscript was partially funded by the Deutsche Forschungsgemeinschaft (DFG, German Research Foundation) – Project-ID 424778381 – TRR 295.

REFERENCES

[1] W. Schuepbach, J. Rau, K. Knudsen, J. Volkmann, P. Krack, L. Timmermann, T. Hälbig, H. Hesekamp, S. Navarro, N. Meier *et al.*, "Neurostimulation for Parkinson's disease with early motor complications," *New England Journal of Medicine*, vol. 368, no. 7, pp. 610–622, 2013.

[2] G. Deuschl, C. Schade-Brittinger, P. Krack, J. Volkmann, H. Schäfer, K. Bötzel, C. Daniels, A. Deutschländer, U. Dillmann, W. Eisner *et al.*, "A randomized trial of deep-brain stimulation for Parkinson's disease," *New England Journal of Medicine*, vol. 355, no. 9, pp. 896–908, 2006.

[3] M. L. Janssen, A. A. Duits, A. M. Tourai, L. Ackermans, A. F. Leentjes, V. van Kranen-Mastenbroek, M. Oosterloo, V. Visser-Vandewalle, and Y. Temel, "Subthalamic nucleus high-frequency stimulation for advanced Parkinson's disease: motor and neuropsychological outcome after 10 years," *Stereotactic and functional neurosurgery*, vol. 92, no. 6, pp. 381–387, 2014.

[4] K. Witt, C. Daniels, and J. Volkmann, "Factors associated with neuropsychiatric side effects after STN-DBS in Parkinson's disease," *Parkinsonism & related disorders*, vol. 18, pp. S168–S170, 2012.

[5] D. Mücke, A. Hermes, T. B. Roettger, J. Becker, H. Niemann, T. A. Dembek, L. Timmermann, V. Visser-Vandewalle, G. R. Fink, M. Grice *et al.*, "The effects of thalamic deep brain stimulation on speech dynamics in patients with essential tremor: An articulographic study," *PLoS One*, vol. 13, no. 1, p. e0191359, 2018.

[6] H. Cagnan, T. Denison, C. McIntyre, and P. Brown, "Emerging technologies for improved deep brain stimulation," *Nature biotechnology*, vol. 37, no. 9, pp. 1024–1033, 2019.

[7] S. Little, A. Pogosyan, S. Neal, B. Zavala, L. Zrinzo, M. Hariz, T. Foltynie, P. Limousin, K. Ashkan, J. FitzGerald, A. L. Green, T. Z. Aziz, and P. Brown, "Adaptive deep brain stimulation in advanced Parkinson disease," *Annals of Neurology*, vol. 74, no. 3, pp. 449–457, sep 2013.

[8] A. Priori, G. Foffani, L. Rossi, and S. Marceglia, "Adaptive deep brain stimulation (aDBS) controlled by local field potential oscillations," *Experimental neurology*, vol. 245, pp. 77–86, 2013.

[9] S. E. Qasim, C. de Hemptinne, N. C. Swann, S. Miocinovic, J. L. Ostrem, and P. A. Starr, "Electrocorticography reveals beta desynchronization in the basal ganglia-cortical loop during rest tremor in Parkinson's disease," *Neurobiology of disease*, vol. 86, pp. 177–186, 2016.

[10] P. Fischer, W. J. Lipski, W.-J. Neumann, R. S. Turner, P. Fries, P. Brown, and R. M. Richardson, "Movement-related coupling of human subthalamic nucleus spikes to cortical gamma," *Elife*, vol. 9, p. e51956, 2020.

[11] E. D. Kondylis, M. J. Randazzo, A. Alhourani, W. J. Lipski, T. A. Wozny, Y. Pandya, A. S. Ghuman, R. S. Turner, D. J. Crammond, and R. M. Richardson, "Movement-related dynamics of cortical oscillations in Parkinson's disease and essential tremor," *Brain*, vol. 139, no. 8, pp. 2211–2223, 2016.

[12] N. C. Swann, C. de Hemptinne, M. C. Thompson, S. Miocinovic, A. M. Miller, J. L. Ostrem, H. J. Chizeck, P. A. Starr *et al.*, "Adaptive deep brain stimulation for Parkinson's disease using motor cortex sensing," *Journal of neural engineering*, vol. 15, no. 4, p. 046006, 2018.

[13] W. J. Neumann, R. S. Turner, B. Blankertz, T. Mitchell, A. A. Kühn, and R. M. Richardson, "Toward Electrophysiology-Based Intelligent Adaptive Deep Brain Stimulation for Movement Disorders," *Neurotherapeutics*, vol. 16, no. 1, pp. 105–118, 2019.

[14] S. Castaño-Candamil, B. I. Ferleger, A. Haddock, S. S. Cooper, J. Herron, A. Ko, H. J. Chizeck, and M. Tangermann, "A Pilot Study on Data-Driven Adaptive Deep Brain Stimulation in Chronically Implanted Essential Tremor Patients," *Frontiers in Human Neuroscience*, vol. 14, p. 541625, nov 2020.

[15] B. I. Ferleger, B. Houston, M. C. Thompson, S. S. Cooper, K. S. Sonnet, A. L. Ko, J. A. Herron, and H. J. Chizeck, "Fully implanted adaptive deep brain stimulation in freely moving essential tremor patients," *Journal of Neural Engineering*, vol. 17, no. 5, p. 056026, oct 2020.

[16] R. Gilron, S. Little, R. Perrone, R. Wilt, C. de Hemptinne, M. S. Yaroshinsky, C. A. Racine, S. S. Wang, J. L. Ostrem, P. S. Larson, D. D. Wang, N. B. Galifianakis, I. O. Bledsoe, M. San Luciano, H. E. Dawes, G. A. Worrell, V. Kremen, D. A. Borton, T. Denison, and P. A. Starr, "Long-term wireless streaming of neural recordings for circuit discovery and adaptive stimulation in individuals with Parkinson's disease," *Nature Biotechnology*, 2021.

[17] F. Lotte, L. Bougrain, A. Cichocki, M. Clerc, M. Congedo, A. Rakotomamonjy, and F. Yger, "A review of classification algorithms for EEG-based brain–computer interfaces: a 10 year update," *Journal of neural engineering*, vol. 15, no. 3, p. 031005, 2018.

[18] A. C. Meidahl, G. Tinkhauser, D. M. Herz, H. Cagnan, J. Debarros, and P. Brown, "Adaptive deep brain stimulation for movement disorders: the long road to clinical therapy," *Movement disorders*, vol. 32, no. 6, pp. 810–819, 2017.

[19] S. He, J. Debarros, S. Khawaldeh, A. Pogosyan, A. Mostofi, F. Baig, E. Pereira, P. Brown, and H. Tan, "Closed-loop DBS triggered by real-time movement and tremor decoding based on thalamic LFPs for essential tremor," in *Proceedings of the Annual International Conference of the IEEE Engineering in Medicine and Biology Society, EMBS*, vol. 2020-July. Institute of Electrical and Electronics Engineers Inc., jul 2020, pp. 3602–3605.

[20] E. Opri, S. Cernera, R. Molina, R. S. Eisinger, J. N. Cagle, L. Almeida, T. Denison, M. S. Okun, K. D. Foote, and A. Gunduz, "Chronic embedded cortico-thalamic closed-loop deep brain stimulation for the treatment of essential tremor," *Science Translational Medicine*, 2020.

[21] T. Merk, V. Peterson, W. Lipski, B. Blankertz, R. S. Turner, N. Li, A. Horn, A. A. Kühn, R. M. Richardson, and W.-J. Neumann, "Electrocorticography is superior to subthalamic local field potentials for movement decoding in Parkinson's disease," *bioRxiv*, 2021.

[22] K. K. Ang, Z. Y. Chin, H. Zhang, and C. Guan, "Filter bank common spatial pattern (FBCSP) in brain-computer interface," in *2008 IEEE International Joint Conference on Neural Networks (IEEE World Congress on Computational Intelligence)*. IEEE, 2008, pp. 2390–2397.

[23] V. Peterson, D. Wyser, O. Lambercy, R. Spies, and R. Gassert, "A penalized time-frequency band feature selection and classification procedure for improved motor intention decoding in multichannel EEG," *Journal of neural engineering*, vol. 16, no. 1, p. 016019, 2019.

[24] D. Sabbagh, P. Ablin, G. Varoquaux, A. Gramfort, and D. A. Engemann, "Predictive regression modeling with MEG/EEG: from source power to signals and cognitive states," *NeuroImage*, p. 116893, 2020.

[25] S. Dähne, F. C. Meinecke, S. Haufe, J. Höhne, M. Tangermann, K. R. Müller, and V. V. Nikulin, "SPoC: A novel framework for relating the amplitude of neuronal oscillations to behaviorally relevant parameters," *NeuroImage*, vol. 86, no. September, pp. 111–122, 2014.

[26] S. Castaño-Candamil, T. Piroth, P. Reinacher, B. Sajonz, V. A. Coenen, and M. Tangermann, "Identifying controllable cortical neural markers with machine learning for adaptive deep brain stimulation in Parkinson's disease," *NeuroImage: Clinical*, vol. 28, p. 102376, 2020.

[27] E. D. Kondylis, M. J. Randazzo, A. Alhourani, W. J. Lipski, T. A. Wozny, Y. Pandya, A. S. Ghuman, R. S. Turner, D. J. Crammond, and R. M. Richardson, "Movement-related dynamics of cortical oscillations in Parkinson's disease and essential tremor," *Brain*, vol. 139, no. 8, pp. 2211–2223, 2016.

[28] N. D. Sisterson, A. A. Carlson, U. Rutishauser, A. N. Mamelak, M. Flagg, N. Pouratian, Y. Salimpour, W. S. Anderson, and R. M. Richardson, "Electrocorticography during deep brain stimulation surgery: safety experience from 4 centers within the national institute of neurological disorders and stroke research opportunities in human consortium," *Neurosurgery*, vol. 88, no. 5, pp. E420–E426, 2021.

[29] Z. Xie, O. Schwartz, and A. Prasad, "Decoding of finger trajectory from ECoG using deep learning," *Journal of Neural Engineering*, vol. 15, no. 3, 2018.

[30] S. Baillet, J. C. Mosher, and R. M. Leahy, "Electromagnetic brain mapping," *IEEE Signal processing magazine*, vol. 18, no. 6, pp. 14–30, 2001.

[31] L. C. Parra, C. D. Spence, A. D. Gerson, and P. Sajda, "Recipes for the linear analysis of EEG," *Neuroimage*, vol. 28, no. 2, pp. 326–341, 2005.

[32] A. de Cheveigné and L. C. Parra, "Joint decorrelation, a versatile tool for multichannel data analysis," *Neuroimage*, vol. 98, pp. 487–505, 2014.

[33] J. Snoek, H. Larochelle, and R. P. Adams, "Practical Bayesian optimization of machine learning algorithms," in *Proceedings of the 25th International Conference on Neural Information Processing Systems-Volume 2*, 2012, pp. 2951–2959.

[34] A. Gramfort, M. Luessi, E. Larson, D. A. Engemann, D. Strohmeier, C. Brodbeck, R. Goj, M. Jas, T. Brooks, L. Parkkonen *et al.*, "MEG and EEG data analysis with MNE-Python," *Frontiers in neuroscience*, vol. 7, p. 267, 2013.

[35] M. Jas, T. Achakulvisut, A. Idrizović, D. Acuna, M. Antalek, V. Marques, T. Odland, R. Garg, M. Agrawal, Y. Umegaki, P. Foley, H. Fernandes, D. Harris, B. Li, O. Pieters, S. Otterson, G. D. Toni, C. Rodgers, E. Dyer, M. Hamalainen, K. Kording, and P. Ramkumar, "Pyglmnet: Python implementation of elastic-net regularized generalized linear models," *Journal of Open Source Software*, vol. 5, no. 47, p. 1959, 2020.

[36] V. Jayaram and A. Barachant, "MOABB: trustworthy algorithm benchmarking for BCIs," *Journal of neural engineering*, vol. 15, no. 6, p. 066011, 2018.

[37] F. Pedregosa, G. Varoquaux, A. Gramfort, V. Michel, B. Thirion, O. Grisel, M. Blondel, P. Prettenhofer, R. Weiss, V. Dubourg, J. Vanderplas, A. Passos, D. Cournapeau, M. Brucher, M. Perrot, and E. Duchesnay, "Scikit-learn: Machine learning in Python," *Journal of Machine Learning Research*, vol. 12, pp. 2825–2830, 2011.

[38] F. Nogueira, "Bayesian Optimization: Open source constrained global optimization tool for Python," 2014–.

[39] J. G. Proakis, *Digital signal processing: principles algorithms and applications*. Pearson Education India, 2001.

[40] S. A. Shah, H. Tan, G. Tinkhauser, and P. Brown, "Towards real-time, continuous decoding of gripping force from deep brain local field potentials," *IEEE Transactions on Neural Systems and Rehabilitation Engineering*, vol. 26, no. 7, pp. 1460–1468, 2018.

[41] S. Haufe, F. Meinecke, K. Görgen, S. Dähne, J.-d. Haynes, B. Blankertz, and F. Bießmann, "NeuroImage On the interpretation of weight vectors of linear models in multivariate neuroimaging," *NeuroImage*, vol. 87, pp. 96–110, 2014.

[42] F. Panov, E. Levin, C. de Hemptinne, N. C. Swann, S. Qasim, S. Miocinovic, J. L. Ostrem, and P. A. Starr, "Intraoperative electrocorticography for physiological research in movement disorders: principles and experience in 200 cases," *Journal of neurosurgery*, vol. 126, no. 1, pp. 122–131, 2017.

[43] T. Jiang, T. Jiang, T. Wang, S. Mei, Q. Liu, Y. Li, X. Wang, S. Prabhu, Z. Sha, and N. F. Ince, "Characterization and decoding the spatial patterns of hand extension/flexion using high-density ECoG," *IEEE Transactions on Neural Systems and Rehabilitation Engineering*, vol. 25, no. 4, pp. 370–379, 2017.

[44] S. Castaño-Candamil, T. Piroth, P. Reinacher, B. Sajonz, V. A. Coenen, and M. Tangermann, "Identifying controllable cortical neural markers with machine learning for adaptive deep brain stimulation in Parkinson's disease," *NeuroImage: Clinical*, vol. 28, no. August, p. 102376, 2020.